An all-in-one numerical methodology for fretting wear and fatigue life assessment

I. Llavori
Departamento de Mecánica y Producción Industrial,
Escuela Politécnica Superior de Mondragon Unibertsitatea, Loramendi 4, 20500, Arrasate-Mondragon, Spain,
illavori@mondragon.edu

M.A. Urchegui
Orona EIC, Orona Ideo, Jauregi bidea s/n, 20120, Hernani, Spain,
maurchegui@orona-group.com

W. Tato, X. Gomez
Departamento de Mecánica y Producción Industrial,
Escuela Politécnica Superior de Mondragon Unibertsitatea, Loramendi 4, 20500, Arrasate-Mondragon, Spain,
wtato@mondragon.edu, xgomez@mondragon.edu

ABSTRACT. Many mechanical components such as, bearing housings, flexible couplings and spines or orthopedic devices are simultaneously subjected to a fretting wear and fatigue damage. For this reason, the combined study on a single model of wear, crack initiation and propagation is of great interest. This paper presents an all-in-one 2D cylinder on flat numerical model for life assessment on coupled fretting wear and fatigue phenomena. In the literature, two stages are usually distinguished: crack nucleation and its subsequent growth. The method combines the Archard wear model, a critical-plane implementation of the Smith-Watson-Topper (SWT) multiaxial fatigue criterion coupled with the Miner-Palmgren accumulation damage rule for crack initiation prediction. Then, the Linear Elastic Fracture Mechanics (LEFM) via eXtended Finite Element Method (X-FEM) embedded into the commercial finite element code Abaqus FEA has been employed to determine the crack propagation stage. Therefore, the sum of the two stages gives a total life prediction. Finally, the numerical model was validated with experimental data reported in the literature and a good agreement was obtained.

KEYWORDS. Fretting; Multiaxial Fatigue; Wear; Crack Propagation; X-FEM.

INTRODUCTION

Many mechanical components such as, bearing housings, flexible couplings and spines or orthopedic devices are simultaneously subjected to a fretting wear and fatigue damage. Fretting phenomenon arises when two bodies are in contact subjected to relative movement of small amplitude, producing damage to the contact surface [1]. Depending on the magnitude of stresses, fretting phenomenon can cause catastrophic failure of such mechanical components.

In general, the study of fretting is divided into two stages, the crack initiation and its subsequent propagation. On the one hand, due to the non-proportional multiaxial state of contact stress field, the use of multiaxial fatigue parameters has become a very popular technique for fatigue life assessment [2]. On the other hand, several studies analyses the propagation phase in terms of the Linear Elastic Fracture Mechanics (LEFM) for brittle materials. In this regard, works such as Vázquez [3] employs analytical methods to estimate cycles to failure. Other works like the one of Giner *et al.* [4] studies the mechanics of the contact in presence of a crack in a single numerical model due to the advantage of the eXtended Finite Element Method (X-FEM) [5]. However, these studies are mainly focused in the partial slip regime where the removal of material is not important and therefore, do not need to employ wear simulation techniques.
In the presence of wear, one of the most prominent works is presented by Madge *et al.* [6]. First, the numerical simulation of the process of material removal using the Abaqus FEA user subroutine UMESHMOTION is performed. Then, crack initiation analysis using the Smith-Watson-Topper (SWT) multiaxial fatigue parameter coupled with the Miner-Palmgren accumulation damage framework to account the effect of wear is carried out. Finally, the propagation phase is analyzed via submodelling technique. This method allows to transfer the stress state of the contact surface from global wear model to crack submodel. Consequently, the explicit interaction between the fretting contact and the crack can't be modelled.
The aim of this paper is to employ the X-FEM methodology implemented by Giner *et al.* [4] to explicitly model the interaction between the fretting contact and the crack, to explain the same set of numerical problems analyzed by Madge *et al.* [4.] Therefore, the developed method combines the Archard wear model, a critical-plane implementation of the SWT multiaxial fatigue criterion coupled with the Miner-Palmgren accumulation damage rule for crack initiation prediction, and the X-FEM developed by Giner *et al.* [7] in addition to the Level Set Method (LSM) [8] in order to detect the extended elements, for crack propagation prediction. Therefore, the sum of the two stages gives a total life prediction.

REVIEW OF WEAR, CRACK INITIATION AND PROPAGATION CRITERIA

Wear law criterion

The wear simulation algorithm used in this work is the one presented by McColl et al. [9] for 2D numerical model and used also by Cruzado et al. [10] for 3D simulations. The simulation methodology is based on the Archard wear law, an iterative process in which the local Archard equation is resolved by means of the finite element contact stresses and slip distribution results. However, this process requires a high computational performance, therefore the cycle jump technique is employed [9,10], where it is made the assumption that wear remains constant over a small number of cycles. Thus, the Archard local equation (Eq. 1) is defined as

$$\Delta h(x,t)=\Delta n\times k\times p(x,t)\times\Delta s(x,t) \tag{1}$$

where $\Delta h(x,t)$, Δn, k, $p(x,t)$ y $\Delta s(x,t)$ are the incremental wear depth, the cycle jump, Archard wear coefficient, the contact pressure and the relative slip for a specific point at specific time.
The wear coefficient used in this work is based on the experimental results of Magaziner et al. [11] which was estimated by McColl et al. [9] and employed later by Madge et al. [6].

Crack Nucleation Criteria

As it has been mentioned in the introduction, due to the non-proportional multiaxial state of stress field, the use of multiaxial fatigue parameters has become a popular technique. In this paper the SWT (Eq. 2) criterion [12] is used to predict the location, plane and cycles to crack nucleation.

$$\mathrm{SWT}=\left(\sigma_{\max}\frac{\Delta\varepsilon}{2}\right)_{\max}=\frac{\sigma'^{2}_{\mathrm{f}}}{E}\left(2N_{\mathrm{f}}\right)^{2b}+\sigma'_{\mathrm{f}}\varepsilon'_{\mathrm{f}}\left(2N_{\mathrm{f}}\right)^{b+c} \tag{2}$$

where σ_f' is the fatigue strength coefficient, ε_f' is the fatigue ductility coefficient, b is the fatigue strength exponent and c is the fatigue ductility exponent. The fatigue constants used in this paper are the same as the ones employed by Madge et al. [6].
The stress state in the contact zone varies during the test due to wear phenomenon, thereby the SWT value is different for each wear state. One of the most commonly used techniques to take into account these states is the damage accumulation rule of Miner-Palmgren (Eq. 3), defined as

$$\omega = \sum_{i=1}^{k} \frac{n_i}{N_i}, \tag{3}$$

where ω is the total accumulated damage (nucleation is defined to have occurred when the parameter reaches the value of 1), n_i is the number of cycle completed in each wear stress state and N_i is the theoretical number of cycles to failure predicted by the SWT parameter for each wear stress state. In this paper, the implementation of the Miner's rule presented by Cruzado *et al.* [13] has been employed.

Crack Propagation Criteria

To estimate the second phase of the presented method, a crack growth law of the type $da/dN = f(\Delta K)$ based on the LEFM has been used to determine the crack propagation rate. The model relies the correct calculation of the Stress Intensity Factor (SIF) on the X-FEM, using the J integral through the interaction integral. Thus, the effect of the crack/fretting-contact evolution can be analyzed in a single numerical model as shown by Giner *et al.* [4]. The fracture constants used in this paper are the same as the ones employed by Madge *et al.* [6]. In this work, it is assumed that the crack propagation takes place under mode I, e.g. $\Delta K = K_{I\,max}$, since $K_{I\,min}$ is almost 0 due to stress ratio being R = 0.03 and perpendicular to the initial contact surface.

EXPERIMENTAL TEST DESCRIPTION

The fretting fatigue experimental tests selected for comparison purpose is reported in the literature by Magaziner *et al.* [11]. The test machine shown in Fig. 1 consists of two servo-hydraulic actuators. The main actuator controlled the alternating axial load (σ) of the fatigue specimen, while the secondary actuator controlled the tangential load (Q). Thus, the test machine is capable to perform a combined fretting fatigue and wear test. The selected tests are 9A and 10A, and the amplitude of displacement between the fretted bodies are δ = 36 μm and δ = 104 μm respectively.

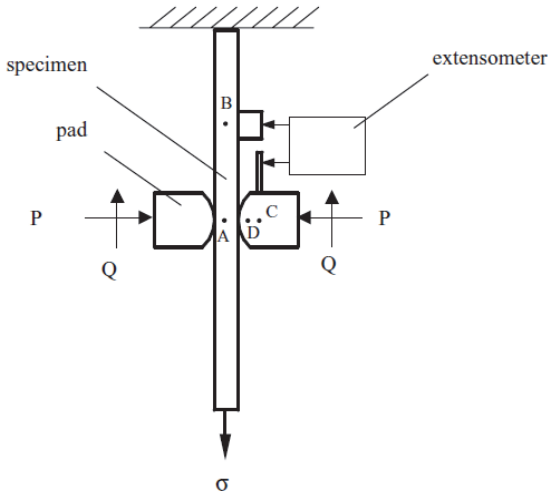

Figure 1: Schematic of cylinder on flat fretting fatigue test configuration [11].

NUMERICAL MODEL

The model shown in Fig. 2 has been developed in the commercial code Abaqus FEA. Due to the typical fretting fatigue testing geometry, half the specimen has been modelled as in references [2,3,4,6]. The model consists of linear quadrilateral elements of 4 nodes (CPE4), with further refinement on the contact neighborhood by the partition technique. In order to obtain a precise slip distribution, the Coulomb and the Lagrange multipliers methods have been used to model the tangential contact. Fig. 3 shows the developed coupled wear, crack initiation and crack propagation numerical flow chart.

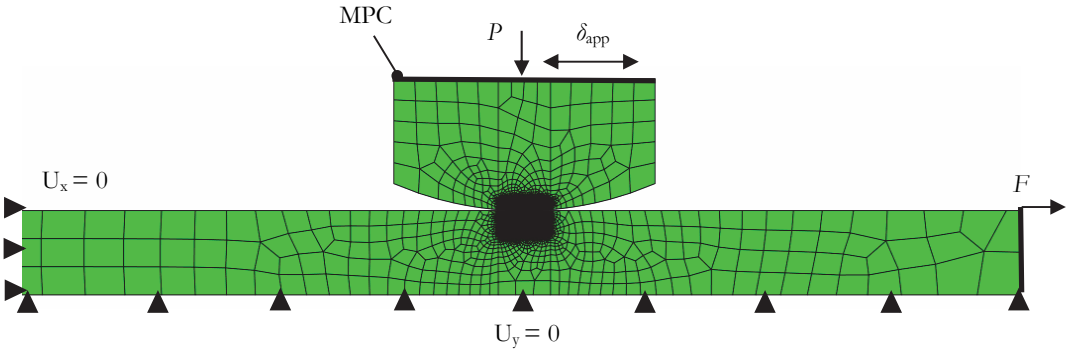

Figure 2: Boundary condition of the numerical model.

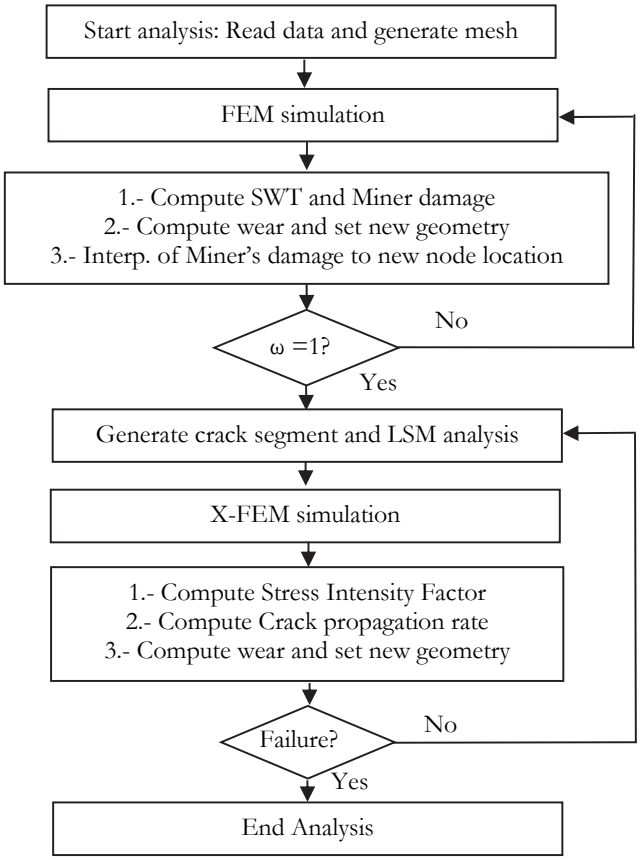

Figure 3: Flow chart showing computational sequence for numerical analysis.

RESULTS

Fig. 7 illustrates the evolution of the Von Mises (VM) stress field at different stages of the δ = 36 μm amplitude displacement simulation (Test 9A), when the maximum axial load is applied. The top left image corresponds to the unworn specimen at the start of the simulation. At this stage, the maximum VM peak stress (1348 MPa) lies at the right end of the contact, that is, on the side where the axial load is applied. The top right figure corresponds to the stress state prior to crack initiation, at 10,000 cycles. It is observed that the contact area is slightly bigger than the initial one, while the reduction of the maximum VM value is around 25% due to the contact stress redistribution originated by wear.

Later, at 20,000 cycles the contact area increases and the right crack lip makes contact, while the crack propagates slowly due to the low value of SIF. It should be mentioned that the black square zone shown in these pictures are the extended elements that represent numerically the crack. Finally, the bottom right figure corresponds to the very end of the simulation, prior to the final rupture of the specimen. At this stage, the contact area remains almost the same, although the stress field changes due to the loss of local stiffness derived from the longer crack.

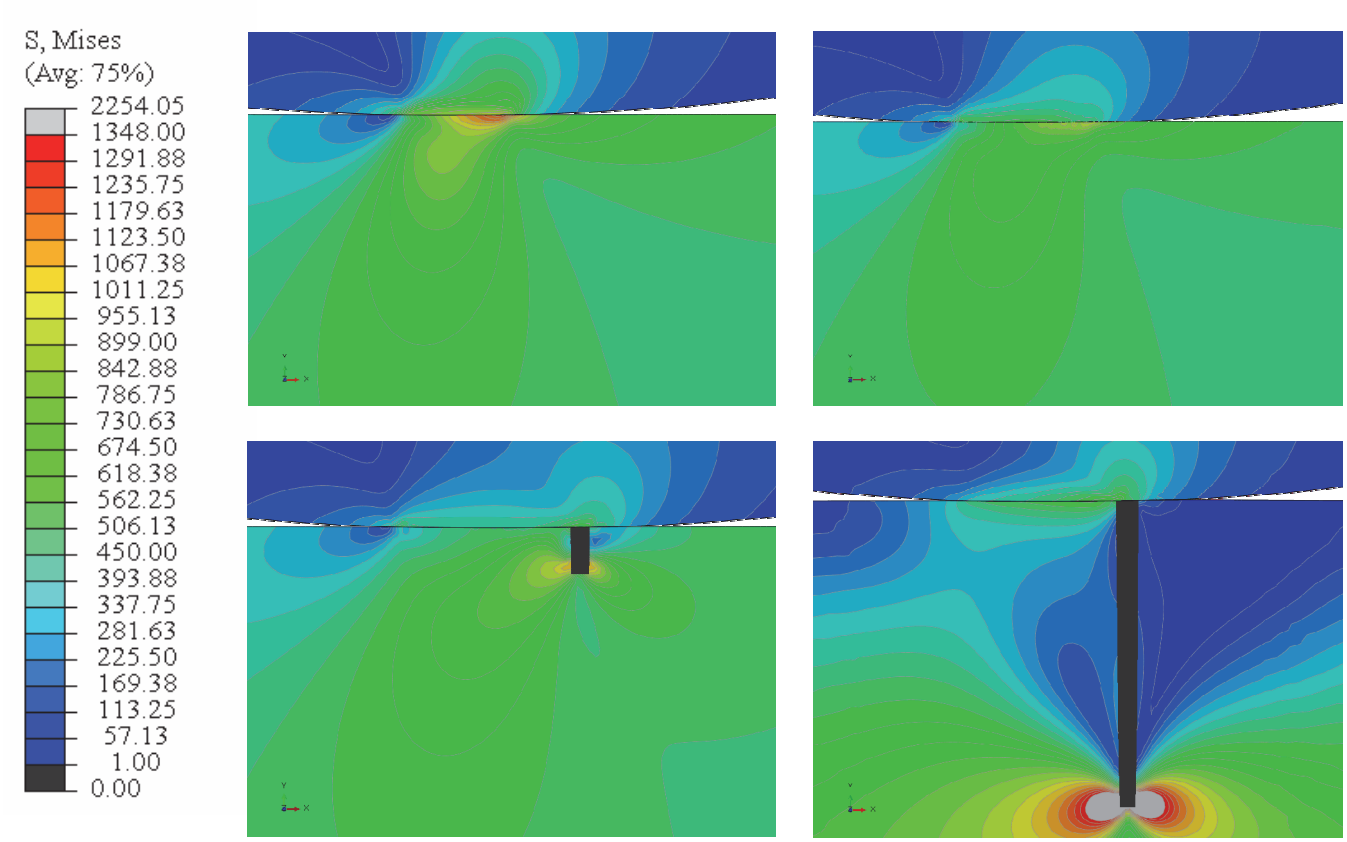

Figure 7: Evolution of the VM stress field at different stages. Top left: Cycle 1; top right: 10,000 cycles; bottom left 20,000 cycles; bottom right 49,300 cycles.

The left side of Fig. 8 shows the Miner's damage evolution for the analyzed cases. On the one hand, the δ = 36 μm displacement amplitude simulation predicts crack nucleation at 10,300 cycles. On the other hand, the δ = 104 μm displacement amplitude simulation predicts no crack nucleation. The later reaches a maximum Miner's damage value of 0.2 at 3,000 cycles and it remains almost constant, with a slight downward slope due to the effect of contact pressure redistribution promoted by the removal of damaged material.

The right side of Fig. 8 shows the SIF range as a function of completed cycles. As expected in the early phase, the crack propagation rate is slow due to the low SIF value. Later, the crack growth rate increases and it propagates until the complete rupture. The fracture toughness (K_{Ic}) of the titanium alloy tested by Magaziner *et al.* (Ti-6Al-4V solution treated and aged), available in the database of materials CES EduPack 2010 [14], is comprehended between 82 and 100 MPa·m$^{1/2}$. The numerical estimation of the fracture toughness value is reached approximately at 52000 cycles. Nevertheless, the ultimate tensile strength (σ_{UTS}) of the titanium alloy is reached before the fracture toughness, therefore it is concluded that the specimen rupture happens at 49300 cycles.

Finally, Tab. 1 shows the comparison between experimental and numerical results. As it can be observed, the numerical model estimations are in very good agreement with the experimental data reported in reference [11].

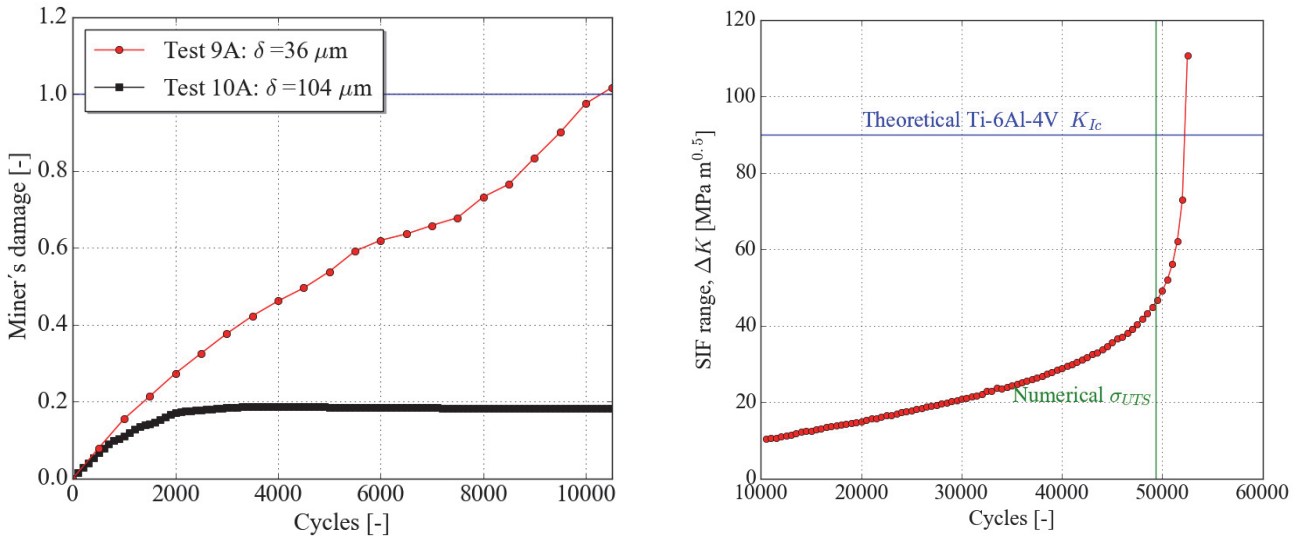

Figure 8: Left side: Detailed view of the Miner's damage evolution to crack initiation. Right side: Estimated SIF range vs. cycles in propagation.

Test	Experimental life	Numerical life prediction
9A (δ = 36 μm)	47,833	49300
10A (δ = 104 μm)	>1,000,000[a]	No crack prediction

[a] Test were stopped after 1 million cycles.

Table 1: Comparison between experimental life and numerical prediction.

Conclusions

In this work, an all-in-one 2D cylinder on flat numerical model that combines wear, crack initiation and propagation has been presented. The numerical results obtained in this work are in a very good agreement with the experimental data reported by Magaziner *et al.* [11].

On the one hand, it has been shown that due to wear simulation the stress field on the fretted bodies changes, depending on the amplitude of displacement. Therefore, it is concluded that the simulation of wear is a key element to assess correctly the life-span of the specimen under gross slip regime.

On the other hand, due to the advantages of the X-FEM, it is possible to study explicitly the interaction between the fretting contact and the existing crack in the presence of wear. In future work, this method will allow to study in great detail the evolution of the fretting contact at different stages under gross slip regime.

Acknowledgements

The authors wish to thank Departamento de Educación, Política Lingüistica y Cultura del Gobierno Vasco for their financial support to the project NUSIMCO (Ref. PI2013-23) through the program "Proyectos de Investigación Básica y/o Aplicada".

References

[1] Vingsbo, O., Soderberg, D., On fretting maps, Wear, 126 (1988) 131-147.

[2] Navarro, C., Muñoz, S., Dominguez, J., On the use of multiaxial fatigue criteria for fretting fatigue life assessment, Int. J. Fatigue, 30 (2008) 32-44.
[3] Vázquez, J., Efecto de las tensiones residuales en la fatiga por fretting. PhD. Thesis, Universidad de Sevilla, Spain, (2009).
[4] Giner, E., Navarro, C., Sabsabi, M., Tur, M., Dominguez, J., Fuenmayor, F.J., Fretting fatigue life prediction using the extended finite element method, Int. J. Fatigue, 53 (2011) 217-225.
[5] Moës, N., Dolbow, J., Belytschko, T., A finite element method for crack growth without remeshing, Int. J. Numer. Meth. Eng., 46(1) (1999) 131-150.
[6] Madge, J.J., Leen, S.B., Shipway, P.H., A combined wear and crack nucleation-propagation methodology for fretting fatigue prediction, Int. J. Fatigue, 30 (2008) 1509-1528.
[7] Giner, E., Sukumar, N., Tarancon, J.E., Fuenmayor, F.J., An Abaqus implementation of the extended finite element method Eng. Fract. Mech., 76 (2009) 347-368.
[8] Stolarska, M., Chopp, D.L., Möes, N., Belytschko, T., Modelling crack growth by level sets in the extended finite element method, Int. J. Numer. Meth. Eng., 51 (2001) 943-960.
[9] McColl, I.R., Ding, J., Leen, S.B., Finite element simulation and experimental validation of fretting wear, Wear, 256 (2004) 1114-1127.
[10] Cruzado, A., Urchegui, M.A., Gómez, X., Finite element modeling and experimental validation of fretting wear scars in thin steel wires, Wear, 289 (2012) 26-38.
[11] Magaziner, R., Jin, O., Mal, S., Slip regime explanation of observed size effects in fretting, Wear, 76 (2004) 347-368.
[12] Socie, D., Marquis, G., Multiaxial Fatigue, SAE Book, Warrendale, (2000).
[13] Cruzado, A., Leen, S.B., Urchegui, M.A., Gómez, X., Finite element simulation of fretting wear and fatigue in thin steel wires, Int. J. Fatigue, 55 (2013) 7-21.
[14] CES EduPack 2010. Granta Design.